

**Role of the  $N^*(1535)$  in  $\eta'$  production**Xu Cao<sup>1,3,\*</sup> and Xi-Guo Lee<sup>1,2,†</sup><sup>1</sup>*Institute of Modern Physics, Chinese Academy of Sciences, Post Office Box 31, Lanzhou 730000, People's Republic of China*<sup>2</sup>*Center of Theoretical Nuclear Physics, National Laboratory of Heavy Ion Collisions, Lanzhou 730000, People's Republic of China*<sup>3</sup>*Graduate School, Chinese Academy of Sciences, Beijing 100049, People's Republic of China*

(Received 2 April 2008; published 30 September 2008)

We study the near-threshold  $\eta'$  production mechanism in nucleon-nucleon and  $\pi N$  collisions under the assumption that subthreshold resonance  $N^*(1535)$  is predominant. In an effective Lagrangian approach that gives a reasonable description to the  $pN \rightarrow pN\eta$  and  $\pi^- p \rightarrow n\eta$  reactions, we find that the excitation of  $N^*(1535)$  resonance from the  $t$ -channel  $\pi$  exchange makes the dominate contribution to the  $pN \rightarrow pN\eta'$  process, and a value of 6.5 for the ratio of  $\sigma(pn \rightarrow pn\eta')$  to  $\sigma(pp \rightarrow pp\eta')$  is predicted. A strongcoupling strength of  $N^*(1535)$  to  $\eta'N$  ( $g_{\eta'NN^*}^2/4\pi = 1.1$ ) is extracted from a combined analysis to  $pp \rightarrow pp\eta'$  and  $\pi N \rightarrow N\eta'$ , and the possible implication to the intrinsic component of  $N^*(1535)$  is explored.

DOI: [10.1103/PhysRevC.78.035207](https://doi.org/10.1103/PhysRevC.78.035207)

PACS number(s): 13.75.Cs, 14.20.Gk

**I. INTRODUCTION**

As the members of the nonet of the lightest pseudoscalar mesons, the  $\eta$  and  $\eta'$  mesons have been the subject of considerable interest since accurate and complete measurements have been performed at the experimental facilities of COSY, MAMI, DISTO, GRAAL, CELSIUS, and SATURNE in the past few years. Their intrinsic structure and properties, as well as the production mechanism in elementary particle and hadron physics, have been intensively explored. The physically observed  $\eta$  and  $\eta'$  mesons are mixtures of the pseudoscalar octet and singlet, which results in a considerable amount of  $s\bar{s}$  in both and accounts for the difference in  $\eta$  mass from that of the pion. The much greater mass of the  $\eta'$  meson is thought to be induced by nonperturbative gluon dynamics [1] and axial anomaly [2].

The  $\eta$  and  $\eta'$  production in nucleon-nucleon ( $NN$ ) collisions strengthens our understanding of those problems and also provides opportunities to study the possible nucleon resonances  $N^*$  that couple only weakly to the pion. From the precise measurements of the total cross section of the  $pp \rightarrow pp\eta$  reaction [3–7], it has been concluded in a number of studies [8–16] that the  $\eta$  meson is dominantly produced through the excitation and de-excitation of the  $N^*(1535)$  resonance in this reaction, though the excitation mechanism is still under debate. The first measurement of the cross section of the quasifree  $pn \rightarrow pn\eta$  reaction [17] shows about a factor of 6.5 larger than that of  $pp \rightarrow pp\eta$ , clearly indicating a dominance of isovector exchange. A recent experimental study of the analyzing power of the  $\bar{p}p \rightarrow pp\eta$  reaction [18] supports the idea that the  $\pi$  meson exchange between the colliding nucleons is predominant. However, the lack of experimentally established baryonic resonances that can decay into  $\eta'$  means that our understanding of  $\eta'$  production is still much poorer and unsatisfactory, and there are only a limited number of studies both experimentally [4,19–22]

and theoretically [23–26]. An early analysis based on the covariant one Boson exchange (OBE) model [24] reproduces the near-threshold total cross section of the  $pp \rightarrow pp\eta'$  reaction without any resonant term. However, a relativistic meson exchange model [25] demonstrates that the existing data could be explained either by mesonic and nucleonic currents or by a dominance of two missing resonances,  $S_{11}(1897)$  and  $P_{11}(1986)$ . The extended study [26] motivated by the updated data of the  $\gamma p \rightarrow \eta' p$  [20] and  $pp \rightarrow pp\eta'$  [21,22] reactions yields resonances  $S_{11}(1650)$  and  $P_{11}(1870)$ , and it is premature to identify these states, as these authors pointed out. Besides, another complication comes from the gluon-induced contact term [27], which would have an extra contribution to the cross section for  $pp \rightarrow pp\eta'$ , since it is possible that  $\eta'$  meson couples strongly to gluon.

Recently, high-precision data of the reaction  $\gamma p \rightarrow \eta' p$  for photon energies from 1.527 to 2.227 GeV have been obtained by the CLAS Collaboration [28], and the analysis [28,29] of these data suggest for the first time that both the  $N^*(1535)$  and  $N^*(1710)$  resonances, known to couple strongly to the  $\eta N$  channel, couple to the  $\eta' N$  channel. Since  $N^*(1535)$  has a nearly 50% branching ratio decaying to  $\pi N$ , this is obviously evidence for the important role of this resonance in the  $\eta'$  near-threshold production. Theoretically,  $N^*(1535)$  is found to be important for the near-threshold  $\Lambda$  and  $\phi$  production in  $NN$  collisions [30], and a significant coupling of  $N^*(1535)$  to strange particles is indicated. Furthermore, the properties of the  $N^*(1535)$  resonance have been extensively discussed within the chiral unitary approach [31], and large couplings to  $\eta N$ ,  $K\Sigma$ , and  $K\Lambda$  have also been illustrated.

Motivated by these research results, in this paper we assume that the excitation and de-excitation of the  $N^*(1535)$  resonance play a major role in  $\eta'$  production in the near-threshold region, and we perform a consistent analysis to the reactions  $pp \rightarrow pp\eta(\eta')$ ,  $pn \rightarrow pn\eta(\eta')$ , and  $\pi N \rightarrow N\eta(\eta')$  in the framework of an effective Lagrangian approach. Because the coupling strength of the  $\eta'$  meson to the nucleon and  $N^*$  are poorly known, in our analysis we do not include  $N^*(1650)$  and  $N^*(1710)$ . In fact,  $N^*(1650)$  seems to couple weakly to the  $\eta' N$  channel, and  $N^*(1710)$ , as a P11 state, couples much

\*caoxu@impcas.ac.cn

†xgl@impcas.ac.cn

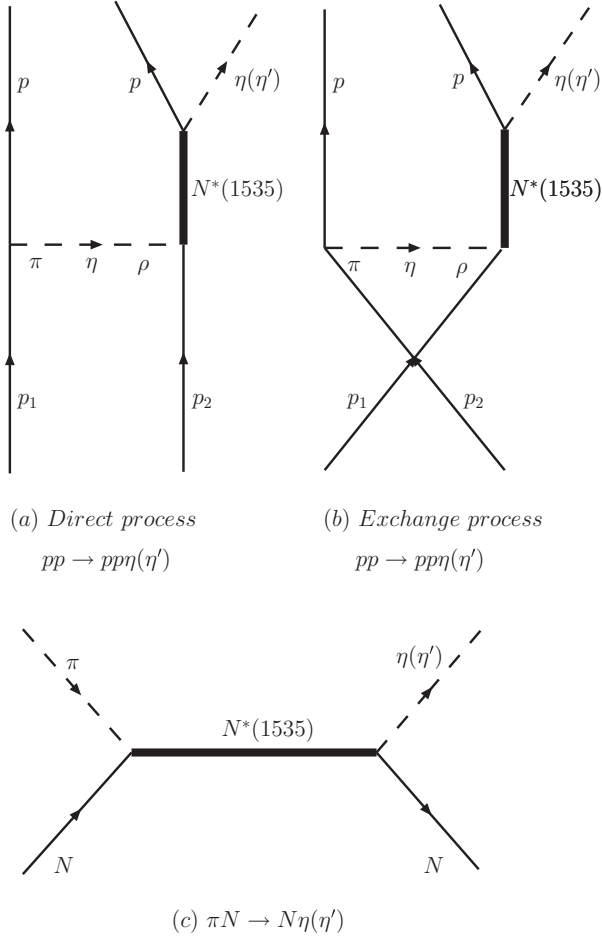


FIG. 1. Feynman diagrams for (a) the direct process  $pp \rightarrow pp\eta(\eta')$ , (b) the exchange process  $pp \rightarrow pp\eta(\eta')$ , and (c)  $\pi N \rightarrow N\eta(\eta')$ .

more weakly to  $\eta'N$  and  $\pi N$  than does  $N^*(1535)$ , so they are expected to make very small contributions to the considered energy region [26,28,29]. The inclusion of the nucleonic and mesonic currents in the intermediate state is found to have a negligible difference on the final results [12,15], so we do not consider them either.

## II. EFFECTIVE LAGRANGIAN APPROACH

We treat the reactions  $pp \rightarrow pp\eta(\eta')$  and  $\pi N \rightarrow N\eta(\eta')$  at the relativistic tree level in an effective Lagrangian approach, as depicted by Feynman diagrams in Fig. 1. Both direct and exchange diagrams [Figs. 1(a) and 1(b)] are considered for

the  $pp \rightarrow pp\eta(\eta')$ , and the dominant s-channel  $N^*(1535)$  resonance [Fig. 1(c)] is included in the  $\pi N \rightarrow N\eta(\eta')$ . Mesons exchanged between the colliding nucleons are restricted to  $\pi$ ,  $\eta$ , and  $\rho$ , which are those observed in the decay channels of the adopted resonances, so most values of the coupling constants are fixed by the experimental decay ratios. As a result, the only adjustable parameters are cutoff parameters in the form factors. All interference terms between different amplitudes are neglected because the relative phases of these amplitudes are not known. The relevant meson-nucleon-nucleon (MNN) and meson-nucleon-resonance (MNR) effective Lagrangians for evaluating the Feynman diagrams in Fig. 1 are [30,32]

$$L_{\pi NN} = -ig_{\pi NN}\bar{N}\gamma_5\vec{\tau} \cdot \vec{\pi}N, \quad (1)$$

$$L_{\rho NN} = -g_{\rho NN}\bar{N}\left(\gamma_\mu + \frac{\kappa}{2m_N}\sigma_{\mu\nu}\partial^\nu\right)\vec{\tau} \cdot \vec{\rho}^\mu N, \quad (2)$$

$$L_{\eta NN} = -ig_{\eta NN}\bar{N}\gamma_5N\eta, \quad (3)$$

$$L_{\pi NN^*} = -g_{\pi NN^*}\bar{N}^*\gamma_5\vec{\tau} \cdot \vec{\pi}N^* + \text{h.c.}, \quad (4)$$

$$L_{\rho NN^*} = ig_{\rho NN^*}\bar{N}^*\gamma_5\left(\gamma_\mu - \frac{q_\mu\gamma \cdot q}{q^2}\right)\vec{\tau} \cdot \vec{\rho}^\mu N^* + \text{h.c.}, \quad (5)$$

$$L_{\eta NN^*} = -g_{\eta NN^*}\bar{N}^*N^*\eta + \text{h.c.}, \quad (6)$$

$$L_{\eta' NN^*} = -g_{\eta' NN^*}\bar{N}^*N^*\eta' + \text{h.c.}, \quad (7)$$

with  $g_{\pi NN}^2/4\pi = 14.4$ ,  $g_{\rho NN}^2/4\pi = 0.9$ , and  $\kappa = 6.1$ . The coupling constant  $g_{\eta NN}$  is undetermined nowadays, and the value of  $g_{\eta NN}^2/4\pi$  used in the literature ranges from 0.25 to 7 [33]. Recent calculations [9,10,13,14,30] seem to favor small  $g_{\eta NN}$ , and  $g_{\eta NN}^2/4\pi = 0.4$  [30] is used in our calculation. The partial decay widths of  $N^*(1535) \rightarrow N\pi$ ,  $N^*(1535) \rightarrow N\rho \rightarrow N\pi\pi$ , and  $N^*(1535) \rightarrow N\eta$  then can be calculated by these Lagrangians, and the coupling constants  $g_{\pi NN^*}^2/4\pi$ ,  $g_{\rho NN^*}^2/4\pi$ , and  $g_{\eta NN^*}^2/4\pi$  are determined through the empirical branching ratios [30,32], as summarized in Table I. Up to now, we have no information on the coupling constant of the  $\eta'NN^*(1535)$  vertex, and we determine it from a combined analysis of  $pp \rightarrow pp\eta'$  and  $\pi N \rightarrow N\eta'$  reactions.

To dampen out high values of the exchanged momentum, the resulting vertexes are multiplied by off-shell form factors. In  $pp \rightarrow pp\eta(\eta')$  reactions, the form factors used in the Bonn model [33] are taken:

$$F_M(q^2) = \left(\frac{\Lambda_M^2 - m_M^2}{\Lambda_M^2 - q_M^2}\right)^n, \quad (8)$$

with  $\Lambda_M$ ,  $q_M$ , and  $m_M$  being, respectively, the cutoff parameter, four-momentum, and mass of the exchanged meson. The commonly used  $n = 2$  for the  $\rho NN$  vertex and  $n = 1$  for other vertexes are employed. The cutoff parameters  $\Lambda_\pi = 1.05$  GeV

TABLE I. Relevant  $N^*(1535)$  parameters.

	Width	Channel	Branching ratio	Adopted value	$g^2/4\pi$
$N^*(1535)$	150 MeV	$\pi N$	0.35–0.55	0.45	0.033
		$\rho N$	$0.02 \pm 0.01$	0.02	0.10
		$\eta N$	0.45–0.60	0.53	0.28
		$\eta' N$	–	–	1.1

for  $\pi NN$ ,  $\Lambda_\rho = 0.92$  GeV for  $\rho NN$ ,  $\Lambda_\eta = 2.00$  GeV for  $\eta NN$ , and  $\Lambda_M = 0.80$  GeV for MNR vertices are adopted from Ref. [32], in which a systematic consistent investigation of the strangeness production process in  $NN$  collisions was performed. In  $\pi N \rightarrow N\eta(\eta')$  reactions, the following form factors for the  $N^*(1535)$  resonance are used [25,26,29,30]:

$$F_{N^*}(q^2) = \frac{\Lambda^4}{\Lambda^4 + (q^2 - M_{N^*}^2)^2}, \quad (9)$$

with the cutoff parameter  $\Lambda = 2$  GeV.

Propagators of  $\pi(\eta)$ ,  $\rho$ , and  $N^*(1535)$  are

$$G_M(q_M) = \frac{i}{q_M^2 - m_M^2}, \quad (10)$$

$$G_\rho^{\mu\nu}(q_\rho) = -i \frac{g^{\mu\nu} - q_\rho^\mu q_\rho^\nu / q_\rho^2}{q_\rho^2 - m_\rho^2}, \quad (11)$$

$$G_R(p_R) = \frac{\gamma \cdot p_R + m_R}{p_R^2 - m_R^2 + im_R \Gamma_R}. \quad (12)$$

With this formalism, the invariant amplitude can be obtained straightforwardly by applying the Feynman rules to Fig. 1.

It is generally agreed that the  $^1S_0$  proton-proton final state interaction (FSI) influences the near-threshold behavior significantly in  $pp \rightarrow pp\eta(\eta')$ . In the present calculation, a Watson-Migdal factorization [34] is used and the  $pp$  FSI enhancement factor is taken to be the Jost function [35]

$$|J(k)|^{-1} = \frac{k + i\beta}{k - i\alpha}, \quad (13)$$

where  $k$  is the internal momentum of the  $pp$  subsystem. The related scattering length  $a$  and effective range  $r$  are

$$a = \frac{\alpha + \beta}{\alpha\beta}, \quad r = \frac{2}{\alpha + \beta}, \quad (14)$$

with  $a = -7.82$  fm and  $r = 2.79$  fm (i.e.,  $\alpha = -20.5$  MeV and  $\beta = 166.7$  MeV) for the  $^1S_0$   $pp$  interaction.

Then the total cross section can be calculated by this prescription, and the integration over the phase space can be performed by a Monte Carlo program. For the  $pn \rightarrow pn\eta(\eta')$  reaction, isospin factors are considered [9,11,15], and  $a = -23.76$  fm and  $r = 2.75$  fm (i.e.,  $\alpha = -7.87$  MeV and  $\beta = 151.4$  MeV) for the  $^1S_0$   $pn$  interaction and  $a = 5.424$  fm and  $r = 1.759$  fm (i.e.,  $\alpha = 45.7$  MeV and  $\beta = 178.7$  MeV) for the  $^3S_1$   $pn$  interaction are used.

In our model, we do not consider initial state interactions (ISI) since it is difficult to treat the ISI unambiguously because so far no accurate  $NN$  interaction model at such high incident beam energies can deal with ISI and FSI simultaneously. Some authors [13] claim that the ISI has practically no influence on the energy dependence of the  $\eta$  production cross section and only leads to a reduction factor of about 0.3 to the cross section in a wide range of energies. In our paper, we do not consider this reduction factor because we do not know the value that we should adopt for the  $\eta'$  production, and so this will just cause another uncertainty. The small cutoff values that we adopt in form factors partly play the role of this reduction factor, and the influence of this prescription will be discussed in the following.

### III. NUMERICAL RESULTS

We first apply our approach to  $\eta$  production and check the applicability of our model. Total cross sections for  $pp \rightarrow pp\eta$ ,  $\pi^- p \rightarrow n\eta$ , and  $pn \rightarrow pn\eta$  are shown in Fig. 2, and our numerical results agree well with the experimental data. The contributions of various meson exchanges to  $pp \rightarrow pp\eta$  and  $pn \rightarrow pn\eta$  are also shown, and  $\pi$  exchange is found to make a dominant contribution in the near-threshold region. This has received support from a recent experiment [18] and is also the reason for our simultaneous reproduction of these two channels [11,15,17]. In sharp contrast to Ref. [9], in which  $\rho$  exchange dominance is indicated, the contribution of  $\rho$  exchange is much smaller than that of  $\pi$  and  $\eta$  exchange in our calculation. Moreover, in a calculation [30] of the  $pp \rightarrow pp\phi$  reaction made with a similar approach to ours, it is demonstrated that the contribution of  $\rho$  exchange is larger than that of  $\eta$  exchange though  $\pi$  exchange is dominant in the  $N^*(1535)$  excitation. This difference from our model is

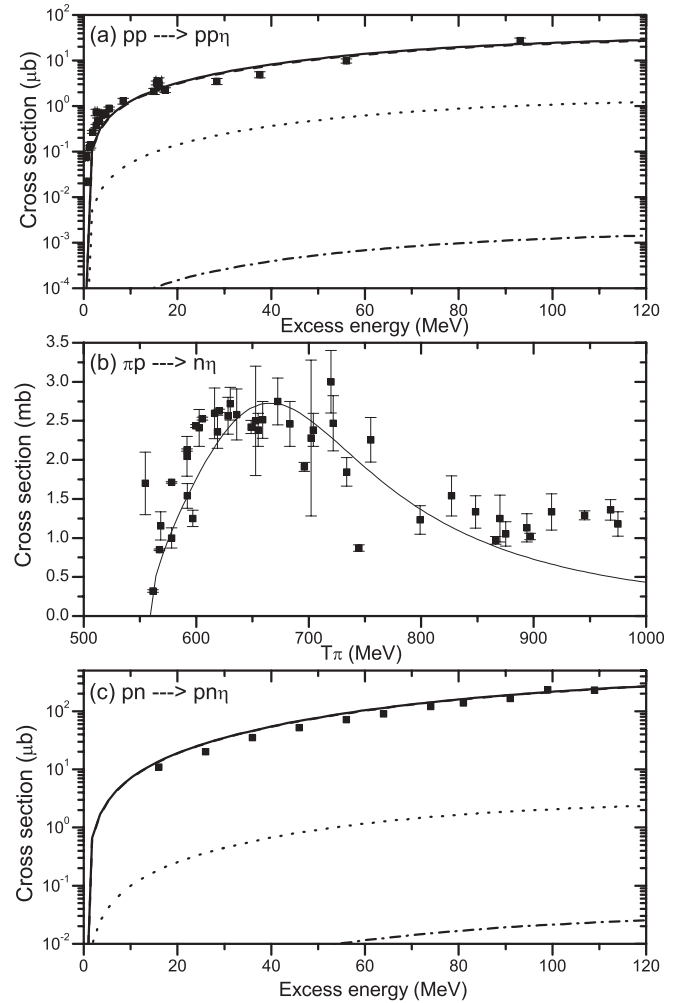


FIG. 2. Total cross section for (a)  $pp \rightarrow pp\eta$ , (b)  $\pi^- p \rightarrow n\eta$ , and (c)  $pn \rightarrow pn\eta$ . In (a) and (c) the dashed, dotted, dash-dotted, and solid curves correspond to contributions from  $\pi$ ,  $\eta$ , and  $\rho$  exchange and their simple sum, respectively. The dashed curve is overlapped by the solid one. The data are from Ref. [3,4] (a), Ref. [36] (b), and Ref. [17] (c).

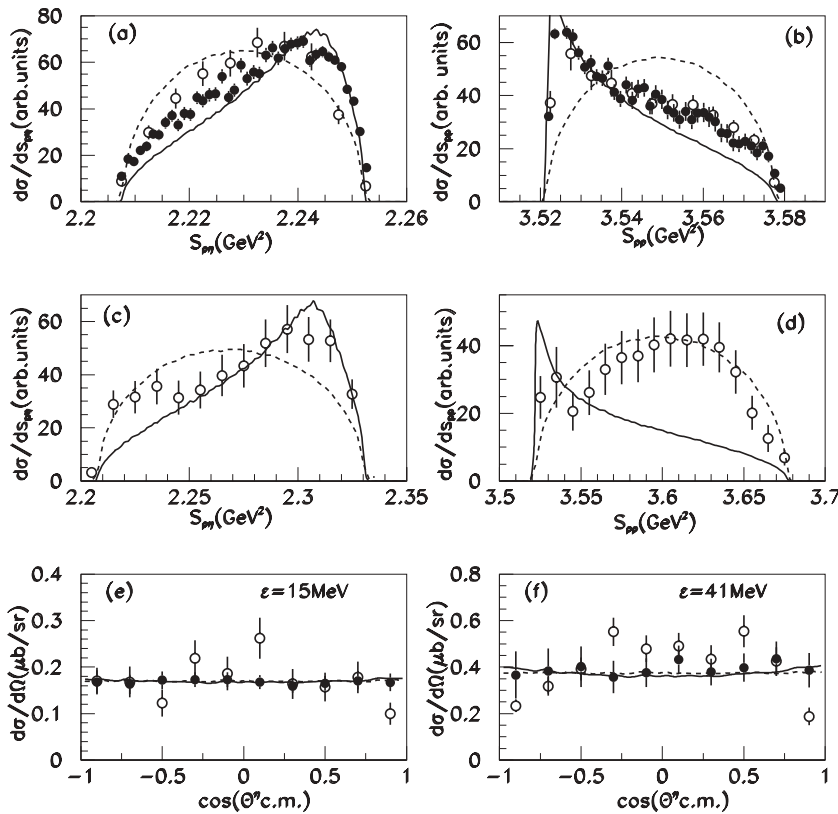


FIG. 3. Invariant mass spectrum for  $pp \rightarrow pp\eta$  at excess energies of (a, b, e) 15 MeV and (c, d, f) 41 MeV. In (a)–(d) the data are from Ref. [6] (open circles) and Ref. [7] (solid circles); in (e) and (f) the data are from Ref. [5] (open circles) and Ref. [6] (solid circles). The dashed curve is the pure phase-space distribution.

caused by the alternative cutoff parameters in the form factors, and much larger values ( $\Lambda = 1.6$  GeV for the  $\rho NN$  vertex and  $\Lambda = 1.3$  GeV for all other form factors) are used in their model. It seems that the vector couplings of the  $\rho NN$  vertex are suppressed more quickly than the pseudoscalar couplings of  $\pi NN$  and  $\eta NN$  vertices when the cutoff parameters are decreased. In the considered energy region, the small cutoff parameters should be more reasonable because we do not include the reduction factor caused by ISI in our model, and these cutoff parameters also give reasonable reproduction of the strangeness production process in  $NN$  collisions [32]. Similarly, our model should draw some analogous conclusions to the  $pN \rightarrow pN\eta'$  channel in this aspect owing to its formalism, as demonstrated in the following. The relatively larger contribution from  $\eta$  exchange compared to that of  $\rho$  exchange is also found in Refs. [11, 14], but it is worth pointing out that a very small  $g_{\eta NN}$  is adopted in our model.

As can be seen from Figs. 2(a) and 2(c), there is not much room left for the coherent resonance-resonance interference term, which is thought to be important, as stressed in Ref. [15]. The cross section of  $\pi^- p \rightarrow n\eta$  when  $T_\pi > 850$  MeV is underestimated, as displayed in Fig. 2(b), and this is obviously evidence of the contribution of other resonances [i.e.,  $N^*(1650)$  and  $N^*(1710)$ ] in this energy region.

For excess energies smaller than 20 MeV, theoretical results underestimate the empirical cross section of the  $pp \rightarrow pp\eta$  channel, as several authors have pointed out [11, 15]. The discrepancy in invariant mass distribution is even more pronounced, as can be clearly seen in Figs. 3(a)–3(d). In addition to a peak arising from the  $N^*(1535)$  resonance and strong  $^1S_0 pp$  FSI, there is a surprising broad bump in both

$pp$  and  $p\eta$  invariant mass distributions, which is not trivially explained. Some papers devote attention to this problem, and the origin of the bump has been attributed to the large  $\eta$  meson exchange contribution comparable with the leading  $\pi$  meson exchange term [14] or higher partial waves [12]. However, the former hypothesis apparently conflicts with the experimental finding of a dominance of isovector exchange; thus it cannot account for the high ratio of  $\sigma(pn \rightarrow pn\eta)$  to  $\sigma(pp \rightarrow pp\eta)$ . The latter cannot give a simultaneous explanation of the excitation function and invariant mass distributions, and the visible bump at excess energies of 4.5 MeV [7] is improbably caused by the contribution of higher partial waves. As a result, it seems that this bump probably arises from the  $\eta N$  FSI [16]. Unfortunately, there has so far been no rigorous treatment of three-pair FSI, and this problem needs further theoretical and experimental effort. As shown in Figs. 3(e) and 3(f), the angular distributions of the  $\eta$  meson in the  $pp \rightarrow pp\eta$  reaction for excess energies of 15 and 41 MeV are described well by our model, since our model is characterized by the  $\pi$  exchange dominance process in the  $N^*(1535)$  excitation.

We will now employ our model to  $\eta'$  production since its success for  $\eta$  production has just been demonstrated. Total cross sections for  $pp \rightarrow pp\eta'$ ,  $\pi N \rightarrow N\eta'$ , and  $pn \rightarrow pn\eta'$  are shown in Fig. 4. We get good reproduction of both  $pp \rightarrow pp\eta'$  and  $\pi N \rightarrow N\eta'$  channels with  $g_{\eta' NN^*}^2/4\pi = 1.1$ , and some similar conclusions to those of  $\eta$  production are achieved as expected.  $\pi$  exchange is the largest contribution in the near-threshold region of  $pN \rightarrow pN\eta'$ , and  $\rho$  exchange is much smaller than  $\pi$  and  $\eta$  exchange. Without complexity caused by  $\eta' N$  interaction [19, 23], our numerical results reproduce the experimental data quite well in the entire energy region

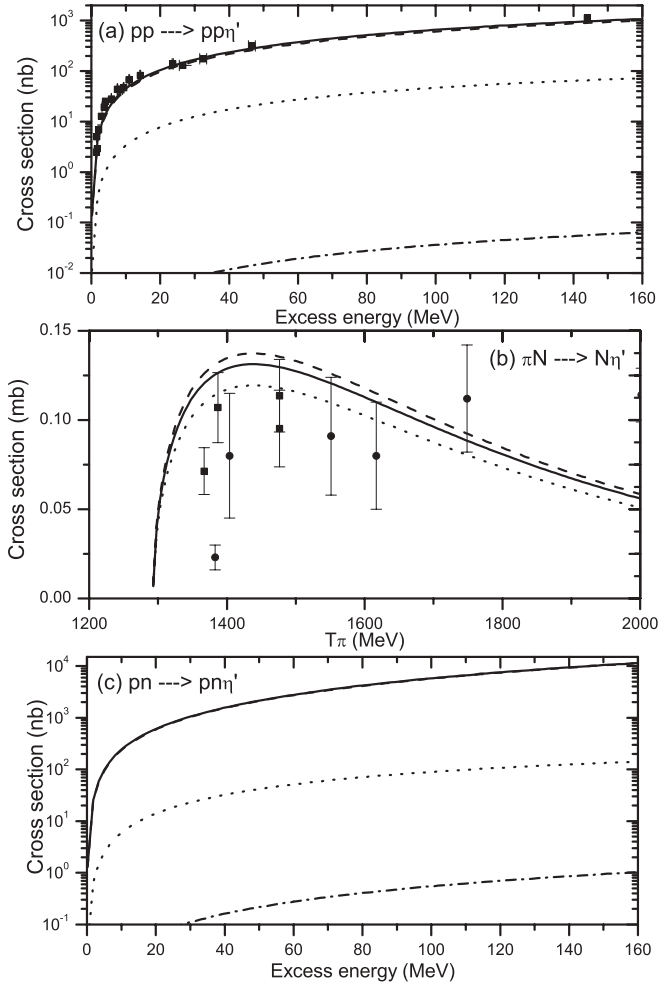


FIG. 4. Total cross section for (a)  $pp \rightarrow pp\eta'$ , (b)  $\pi N \rightarrow N\eta'$ , and (c)  $pn \rightarrow pn\eta'$ (c). In (a) and (c) the dashed, dotted, dash-dotted, and solid curves correspond to contributions from  $\pi$ ,  $\eta$ , and  $\rho$  exchange and their simple sum, respectively. In (b) the dashed, solid, and dotted curves correspond to  $g_{\eta'NN^*}^2/4\pi = 1.15$ , 1.1, and 1.0. The data are from Ref. [19] (a) and Ref. [36] (b) (solid squares:  $\pi^- p \rightarrow n\eta'$ , solid circles:  $\pi^+ n \rightarrow p\eta'$ ).

considered. As can be seen in Fig. 4(c), we anticipate the same value of 6.5 for the ratio of  $\sigma(\pi N \rightarrow N\eta')$  to  $\sigma(pp \rightarrow pp\eta')$  in our model, and this value would approach 4 in the very close to threshold region (excess energy  $< 20$  MeV). This ratio is expected to be unity if  $\eta'$  is produced directly by gluons [27], so isospin dependence is powerful for distinguishing different  $\eta'$  production mechanism and may provide useful information on the possible gluon content of the  $\eta'$  meson.

For the scarce and inaccurate data of  $\pi^- p \rightarrow n\eta'$  and  $\pi^+ n \rightarrow p\eta'$ , the extracted coupling constant  $g_{\eta'NN^*}$  has a large error bar, and significant contributions from other  $N^*$  resonances cannot be definitely excluded. Alternative combinations of  $N^*$  resonances and coupling strength would yield a good fit to the present data [30]. The dotted curve in Fig. 4(b) shows that we can get a much better reproduction of the  $\pi N \rightarrow N\eta'$  data with  $g_{\eta'NN^*}^2/4\pi = 1.0$ , although this will slightly underestimate the  $pp \rightarrow pp\eta'$  channel. An even better fit to the  $pp \rightarrow pp\eta'$  data can be achieved with

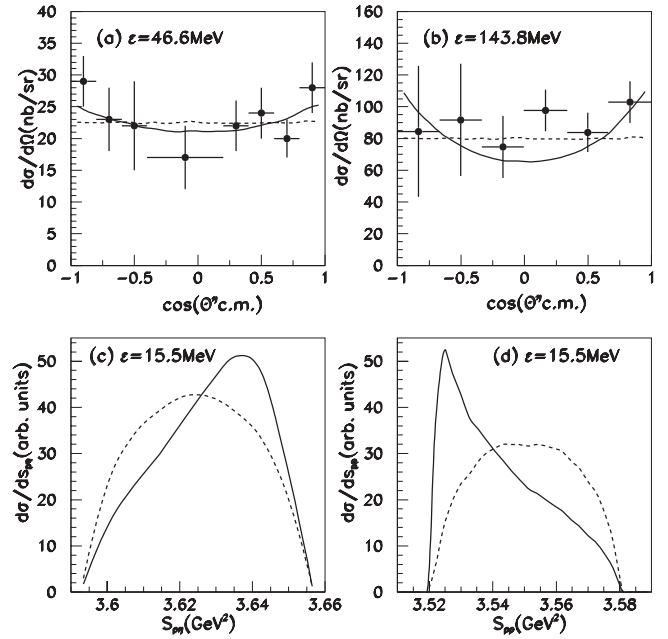


FIG. 5. Invariant mass spectrum for  $pp \rightarrow pp\eta'$ . (a) and (b) show the angular distribution of the  $\eta$  meson and (c) and (d) its invariant mass distribution. The data are from Ref. [22] (a) and Ref. [21] (b). The dashed curve is the pure phase-space distribution.

$g_{\eta'NN^*}^2/4\pi = 1.15$ , but this will overestimate the  $\pi N \rightarrow N\eta'$  data, as shown by the dashed line in Fig 4(b). However, the neglected nucleonic and mesonic currents in the  $pp \rightarrow pp\eta'$  would give an additional contribution, and with a little smaller  $g_{\eta'NN^*}^2/4\pi$  we would achieve a better result for both channels. In any case, our preliminary value of  $g_{\eta'NN^*}^2/4\pi = 1.1$  should be reasonable.

The calculated invariant mass spectrum of the  $pp \rightarrow pp\eta'$  reaction at excess energies of 15.5, 46.6, and 143.8 MeV are presented in Fig. 5. Our calculations of the angular distribution of the  $\eta'$  meson at 46.6 and 143.8 MeV show obvious structure at forward and backward angles and reproduce the experimental data nicely. However, it has to admitted that the measured angular dependence might also be compatible with an isotropic shape within the given experimental uncertainties. Besides, it is interesting to note that the data from Ref. [5] show distinct structure in the angular distribution of the  $\eta$  meson, but Ref. [6] gives a totally flat distribution, as can be seen in Fig. 3(e) and 3(f). So a detailed quantitative analysis awaits more accurate data.

The predicted differential cross section of  $pp \rightarrow pp\eta'$  at an excess energy of 15.5 MeV, together with the total cross section of  $pn \rightarrow pn\eta'$ , can be examined by the ongoing experimental studies [16]. No obvious bump other than a peak arises in the invariant mass distribution because our model does not include additional mechanisms other than the  $N^*(1535)$  resonance and FSI. If this result is confirmed by experiment, then other mechanisms (probably  $\eta N$  FSI) accounting for the broad bump should be added to the study of the  $pp \rightarrow pp\eta'$  channel.

#### IV. SUMMARY AND DISCUSSION

In this paper, we present a consistent analysis of  $pN \rightarrow pN\eta'$  and  $\pi N \rightarrow N\eta'$  within an effective Lagrangian approach, by assuming that the  $N^*(1535)$  resonance is dominant in  $\eta'$  production. Our numerical results show that  $\pi$  exchange is the most important in the  $pN \rightarrow pN\eta'$  reaction, and we predict a large ratio of  $\sigma(pn \rightarrow pn\eta')$  to  $\sigma(pp \rightarrow pp\eta')$ . An explicit structure to the angular distribution of the  $\eta'$  meson is demonstrated. In addition, a significant coupling strength of  $N^*(1535)$  to  $\eta'N$  is found:

$$g_{\eta'NN^*}^2/4\pi = 1.1. \quad (15)$$

In a vector-meson-dominant model analysis to the  $\gamma p \rightarrow p\eta'$  reaction [37], a value of  $g_{\eta'NN^*} = 3.4$  (i.e.,  $g_{\eta'NN^*}^2/4\pi = 0.92$ ) is given, and this is consistent to the result from our analysis. Moreover, the analysis of recent high-precision data for the reaction  $\gamma p \rightarrow p\eta'$  [28,29] gives  $g_{\gamma NN^*}g_{\eta'NN^*} = -2.59$ , and this corresponds to  $g_{\eta'NN^*}^2/4\pi = 1.0$  if we adopt the relation  $g_{\gamma NN^*}^2/4\pi = m_N^2(A_{1/2}^p)^2/[e^2\pi(m_{N^*} - m_N)]$  and the helicity amplitude  $A_{1/2}^p = 0.09 \text{ GeV}^{-1/2}$ . This large coupling strength of  $N^*(1535)$  to  $\eta'N$  is also compatible with the mixture picture of  $\eta$  and  $\eta'$ .

Considering the possible gluonium admixture of the  $\eta'$  wave function, we adopt a basis of states  $|\eta_q\rangle = |u\bar{u} + d\bar{d}\rangle/\sqrt{2}$ ,  $|\eta_s\rangle = |s\bar{s}\rangle$ , and  $|G\rangle = |\text{Gluonium}\rangle$ , and the physical  $\eta$  and  $\eta'$  are assumed to be linear combinations of these basis of states [38,39]:

$$|\eta\rangle = X_\eta|\eta_q\rangle + Y_\eta|\eta_s\rangle + Z_\eta|G\rangle, \quad (16)$$

$$|\eta'\rangle = X_{\eta'}|\eta_q\rangle + Y_{\eta'}|\eta_s\rangle + Z_{\eta'}|G\rangle. \quad (17)$$

If the gluonium content of the  $\eta$  meson is assumed to vanish ( $Z_\eta = 0$ ), all six parameters can be written in terms of two mixing angles,  $\phi_p$  and  $\phi_{\eta'G}$ , which correspond to

$$X_\eta = \cos \phi_p, \quad Y_\eta = -\sin \phi_p, \quad Z_\eta = 0, \quad (18)$$

$$X_{\eta'} = \sin \phi_p \cos \phi_{\eta'G}, \quad Y_{\eta'} = \cos \phi_p \cos \phi_{\eta'G}, \quad (19)$$

$$Z_{\eta'} = -\sin \phi_{\eta'G}.$$

If the gluonium content of the  $\eta'$  meson is further assumed to vanish ( $Z_{\eta'} = 0$ ; i.e.,  $\phi_{\eta'G} = 0$ ), then  $\phi_p$  is the  $\eta$ - $\eta'$  mixing angle in the absence of gluonium, and Eqs. (16) and (17) are the normal  $\eta$ - $\eta'$  mixing in the quark-flavor basis. In the quark model, the  $\eta'$  couplings can be related to those of  $\eta$  [24,37]:

$$g_\eta = X_\eta g_q + Y_\eta g_s + Z_\eta g_G, \quad (20)$$

$$g_{\eta'} = X_{\eta'} g_q + Y_{\eta'} g_s + Z_{\eta'} g_G, \quad (21)$$

with  $g_q$ ,  $g_s$ , and  $g_G$  being, respectively, the nonstrangeness, strangeness, and gluonium coupling constants. For  $g_{\eta'NN}$  and  $g_{\eta NN}$ , because the strangeness and gluonium content in the nucleon are negligible, we can make the simplifying assumption  $g_s \ll g_q$  and  $g_G \ll g_q$  and so

$$R_N = \frac{g_{\eta'NN}}{g_{\eta NN}} \simeq \frac{X_{\eta'}}{X_\eta} = \tan \phi_p \sim 0.84, \quad (22)$$

with  $\phi_p \sim 40^\circ$  [40]. This is compatible with  $R_N \sim 0.62$  from the recently extracted value of  $g_{\eta'NN} \simeq 1.4$  [28] and the adopted value of  $g_{\eta NN}^2/4\pi = 0.4$  in this paper.

With coupling constants summarized in Table I, we have

$$R_{N^*} = \frac{g_{\eta'NN^*}}{g_{\eta NN^*}} \sim 2.0. \quad (23)$$

If the large  $g_{\eta'NN^*}$  indeed indicates a significant  $s\bar{s}$  configuration inside the  $N^*(1535)$  resonance [30], then assuming  $g_{GNN^*} \ll g_{qNN^*}$  should be reasonable, so

$$R_{N^*} = \frac{g_{\eta'NN^*}}{g_{\eta NN^*}} = \frac{\tan \phi_p + g_{sNN^*}/g_{qNN^*}}{1 - g_{sNN^*}/g_{qNN^*} \tan \phi_p}. \quad (24)$$

This gives  $g_{sNN^*}/g_{qNN^*} \sim 0.43$ , which may indicate a relatively large proportion of strangeness in the  $N^*(1535)$  resonance. But the large  $g_{\eta'NN^*}$  is also probably caused by the gluonium component of  $N^*(1535)$ , as can be seen in Eqs. (20) and (21); then if  $g_{sNN^*} \ll g_{qNN^*}$  is assumed, we have

$$R_{N^*} = \frac{g_{\eta'NN^*}}{g_{\eta NN^*}} = \tan \phi_p \cos \phi_{\eta'G} - \frac{g_{GNN^*} \sin \phi_{\eta'G}}{g_{qNN^*} \cos \phi_p}, \quad (25)$$

where  $\phi_p \sim 40^\circ$  and  $|\phi_{\eta'G}| \sim 22^\circ$  [38]. Then we will get  $|g_{GNN^*}/g_{qNN^*}| \sim 2.5$ , and this may also indicate a relatively large proportion of gluons in the  $N^*(1535)$  resonance. Certainly, according to this analysis, it is possible that strangeness and gluons coexist in  $N^*(1535)$ , and it is a combination of them that induces the large couplings of  $N^*(1535)$  to strange particles. Recently, phenomenological analyses of radiative decays and other processes [39] revealed no evidence of the gluonium contribution to the  $\eta'$  wave function (i.e.,  $|\phi_{\eta'G}| \sim 0^\circ$ ), and this seems to support the idea that these large couplings are mainly caused by the  $s\bar{s}$  component in  $N^*(1535)$ . Different five-quark configurations of  $qqqs\bar{s}$  have been deeply investigated, and an admixture of 25%–65% in  $N^*(1535)$  is suggested [41]. However, the intrinsic structure of  $N^*(1535)$  remains an open question and further studies are needed.

In conclusion, our phenomenological analysis of  $\eta'$  production in  $NN$  and  $\pi N$  collisions not only gives a nice reproduction of the experimental data but also agrees well with the present understanding of the internal component of the  $\eta$  ( $\eta'$ ) meson and  $N^*(1535)$  resonance. The ongoing relevant experiment in COSY [16] will soon examine our results and advance a better understanding of  $\eta$  and  $\eta'$  production.

#### ACKNOWLEDGMENTS

We would like to thank Z. Ouyang, Q. W. Wang, J. J. Xie, and B. S. Zou for fruitful discussions and program code. This work was supported by the CAS Knowledge Innovation Project (Nos. KJCX3-SYW-N2 and KJCX2-SW-N16) and the Science Foundation of China (10435080, 10575123, and 10710172).

- [1] G. 't Hooft, Phys. Rev. Lett. **37**, 8 (1976); E. Witten, Nucl. Phys. **B156**, 269 (1979).
- [2] S. L. Adler, Phys. Rev. **177**, 2426 (1969).
- [3] J. Smyrski *et al.*, Phys. Lett. **B474**, 182 (2000); H. Calen *et al.*, Phys. Lett. **B366**, 39 (1996); E. Chiavassa *et al.*, Phys. Lett. **B322**, 270 (1994); A. M. Bergdolt *et al.*, Phys. Rev. D **48**, R2969 (1993); F. Balestra *et al.*, Phys. Rev. C **69**, 064003 (2004).
- [4] F. Hibou *et al.*, Phys. Lett. **B438**, 41 (1998).
- [5] H. Calen *et al.*, Phys. Lett. **B458**, 190 (1999).
- [6] M. Abdel-Bary *et al.*, Eur. Phys. J. A **16**, 127 (2003).
- [7] P. Moskal *et al.*, Phys. Rev. C **69**, 025203 (2004).
- [8] J. M. Laget *et al.*, Phys. Lett. **B257**, 254 (1991); T. Vetter *et al.*, Phys. Lett. **B263**, 153 (1991); M. Batinić *et al.*, Phys. Scr. **56**, 321 (1997); E. Gedalin *et al.*, Nucl. Phys. **A650**, 471 (1999); V. Bernard *et al.*, Eur. Phys. J. A **4**, 259 (1999).
- [9] G. Fäldt and C. Wilkin, Phys. Scr. **64**, 427 (2001).
- [10] M. T. Peña, H. Garcilazo, and D. O. Riska, Nucl. Phys. **A683**, 322 (2001).
- [11] K. Nakayama, J. Speth, and T.-S. H. Lee, Phys. Rev. C **65**, 045210 (2002).
- [12] K. Nakayama, J. Haidenbauer, C. Hanhart, and J. Speth, Phys. Rev. C **68**, 045201 (2003).
- [13] V. Baru, A. M. Gasparyan, J. Haidenbauer, C. Hanhart, A. E. Kudryavtsev, and J. Speth, Phys. Rev. C **67**, 024002 (2003); C. Hanhart and K. Nakayama, Phys. Lett. **B454**, 176 (1999).
- [14] S. Ceci, A. Švarc, and B. Zauner, Phys. Scr. **73**, 663 (2006).
- [15] R. Shyam, Phys. Rev. C **75**, 055201 (2007).
- [16] P. Moskal *et al.*, Int. J. Mod. Phys. A **22**, 305 (2007).
- [17] H. Calen *et al.*, Phys. Rev. C **58**, 2667 (1998).
- [18] R. Czyżykiewicz *et al.*, Phys. Rev. Lett. **98**, 122003 (2007).
- [19] P. Moskal *et al.*, Phys. Rev. Lett. **80**, 3202 (1998); P. Moskal *et al.*, Phys. Lett. **B474**, 416 (2000); P. Moskal *et al.*, Phys. Lett. **B482**, 356 (2000).
- [20] (ABBHHM Collaboration), Phys. Rev. **175**, 1669 (1968); Nucl. Phys. **B108**, 45 (1976); R. Plötzke *et al.*, Phys. Lett. **B444**, 555 (1998); J. Barth *et al.*, Nucl. Phys. **A691**, 374c (2001).
- [21] F. Balestra *et al.*, Phys. Lett. **B491**, 29 (2000).
- [22] A. Khoukaz *et al.*, Eur. Phys. J. A **20**, 345 (2004).
- [23] A. Sibirtsev and W. Cassing, Eur. Phys. J. A **2**, 333 (1998); V. Bernard *et al.*, Eur. Phys. J. A **4**, 259 (1999); V. Baru *et al.*, Eur. Phys. J. A **6**, 445 (1999).
- [24] E. Gedalin, A. Moalem, and L. Razdolskaja, Nucl. Phys. **A650**, 471 (1999).
- [25] K. Nakayama, H. F. Arellano, J. W. Durso, and J. Speth, Phys. Rev. C **61**, 024001 (1999).
- [26] K. Nakayama and H. Haberzettl, Phys. Rev. C **69**, 065212 (2004).
- [27] S. D. Bass, Phys. Lett. **B463**, 286 (1999).
- [28] M. Dugger *et al.*, Phys. Rev. Lett. **96**, 062001 (2006); **96**, 169905(E) (2006).
- [29] K. Nakayama and H. Haberzettl, Phys. Rev. C **73**, 045211 (2006).
- [30] B. C. Liu and B. S. Zou, Phys. Rev. Lett. **96**, 042002 (2006); J. J. Xie, B. S. Zou, and H. C. Chiang, Phys. Rev. C **77**, 015206 (2008).
- [31] N. Kaiser, T. Waas, and W. Weise, Nucl. Phys. **A612**, 297 (1997).
- [32] K. Tsushima, A. Sibirtsev, A. W. Thomas, and G. Q. Li, Phys. Rev. C **59**, 369 (1999).
- [33] R. Machleidt, K. Holinde, and Ch. Elster, Phys. Rep. **149**, 1 (1987).
- [34] K. Watson, Phys. Rev. **88**, 1163 (1952); A. B. Migdal, Sov. Phys. JETP **1**, 2 (1955).
- [35] M. Goldberger, K. M. Watson, *Collision Theory* (Wiley, New York, 1964).
- [36] A. Baldini, V. Flamino, W. G. Moorhead, and D. R. O. Morrison, *Total Cross Sections of High Energy Particles*, Landolt-Bornstein: Numerical Data and Functional Relationships in Science and Technology, vol. 12, edited by H. Schopper (Springer-Verlag, Berlin, 1988).
- [37] A. Sibirtsev, Ch. Elster, S. Krewald, and J. Speth, arXiv:nucl-th/0303044.
- [38] E. Kou, Phys. Rev. D **63**, 054027 (2001); F. Ambrosino *et al.*, Phys. Lett. **B648**, 267 (2007).
- [39] C. E. Thomas, J. High Energy Phys. **10** (2007) 026; R. Escribano, talk presented at the XII International Conference on Hadron Spectroscopy (HADRON 07), Laboratori Nazionali di Frascati (Rome), Italy, 8–13 October 2007, arXiv:hep-ph/0712.1814.
- [40] T. Feldmann and P. Kroll, Eur. Phys. J. C **5**, 327 (1998); (KLOE Collaboration), Phys. Lett. **B541**, 45 (2002).
- [41] B. S. Zou and D. O. Riska, Phys. Rev. Lett. **95**, 072001 (2005); C. S. An and B. S. Zou, arXiv:nucl-th/0802.3996.